ELSEVIER

Physica B 239 (1997) 350–357

PHYSICA B

Magnetic excitations in single crystals of $Cu_{1-x}Ni_xGeO_3$

S. Coad[a,*], O. Petrenko[a], D. McK. Paul[a], B. Fåk[b], J-G. Lussier[c], D.F. McMorrow[c]

[a] *Department of Physics, University of Warwick, Coventry, CV4 7AL, UK*
[b] *SPSMS/MDN/CEA, Grenoble, France*
[c] *Department of Solid State Physics, Risø National Lab, DK-4000 Roskilde, Denmark*

Received 14 December 1996; received in revised form 19 March 1997

Abstract

We have studied magnetic excitations in two single crystals of $CuGeO_3$ doped with Ni^{2+}, using inelastic neutron scattering at wave vectors close to the antiferromagnetic zone centre, $Q=(0,1,\frac{1}{2})$. Pure $CuGeO_3$ is a one-dimensional compound with a spin–Peierls (S–P) gap of ≈ 1.95 meV. When Ni^{2+} is substituted for Cu^{2+} in $CuGeO_3$, the 1D chains are broken into finite segments, suppressing the S–P phase and inducing a low-temperature transition to coexistence with antiferromagnetic order. We show that for the 1.7% Ni-doped crystal the S–P gap is renormalised to ≈ 1.7 meV, while approximate doubling of the dopant concentration to 3.2% results in an almost complete collapse of this excitation. Instead, measurements on the 3.2% Ni-doped crystal revealed a magnetic excitation that could be clearly resolved from the elastic magnetic peak. This excitation followed the dispersion expected for the anisotropy gap in an antiferromagnet and comparison with an equivalent model of the S–P gap in $CuGeO_3$ has yielded modified exchange coefficients. However, measurements could be made only for wave vectors close to $(0,1,\frac{1}{2})$ as the intensity declined rapidly with movement away from the zone centre.

Keywords: Magnetic excitations; $Cu_{1-x}Ni_xGeO_3$

1. Introduction

$CuGeO_3$ is a quasi-one-dimensional (1D) inorganic compound comprised of Cu^{2+} chains along the c-axis. It has recently provoked interest as the first known inorganic substance to undergo a spin–Peierls (S–P) phase transition [1]. A Heisenberg antiferromagnetic 1D chain with $S=\frac{1}{2}$ can reduce its magnetic energy by dimerisation of the lattice along the chain, if the crystal structure can be easily distorted. This dimerisation has been demonstrated in $CuGeO_3$ by the appearance of superlattice peaks at $(h+\frac{1}{2},k,h+\frac{1}{2})$ below 14 K [2]. Exchange coefficients that are unequal and alternate between adjacent sites along the chain lead to the creation of an energy gap separating a singlet ground state from the first excited triplet state. For $CuGeO_3$ there has been an overwhelming weight of experimental evidence [3,4] providing conclusive proof that a spin–Peierls transition does occur in $CuGeO_3$.

In contrast to the previously known organic S–P compounds, $CuGeO_3$ is particularly amenable to the introduction of impurity ions such as Zn^{2+}, Ni^{2+} and Mg^{2+}, onto the Cu^{2+} sites or the replacement of Ge^{4+} ions with Si^{4+} [5,6], Ti^{4+}, Ga^{4+} and many other elements [7]. This has resulted in the proliferation of studies on doped $CuGeO_3$, in the hope of further understanding the mechanism of the S–P transition.

Measurements on doped $CuGeO_3$ show the suppression of T_{sp} and the appearance of a new low-temperature magnetic phase below T_N which has been identified as a 3D antiferromagnetic state [8].

* Corresponding author.

PII S0921-4526(97)00347-5

Doping with different substituents gives qualitatively similar results, in terms of the suppression of T_{sp} and the onset of T_N. In particular, the shape of the phase diagram exhibits an inverted parabolic dependence of T_N on dopant concentration x, regardless of the substituent used. In other words, a maximum T_N exists for a certain x, $\approx 4\%$ for $Cu_{1-x}(Zn/Ni)_xGeO_3$. However, elastic neutron scattering measurements [9, 11] as well as recent susceptibility data [10] show that the direction of the overall magnetic moment in the low-temperature phase does depend upon the substituent – along the c^*-axis for Zn^{2+} ($S=0$) doped samples and in the a^* direction when Ni^{2+} ($S=1$) is introduced. Another feature is the low temperature required to observe the onset of the magnetic order parameter. At present this is attributed to a high degree of magnetic disorder in the lattice [11].

2. Experimental details

We have used inelastic neutron scattering to investigate the magnetic properties of two crystals of $Cu_{1-x}Ni_xGeO_3$, ($x=0.017, 0.032$) at temperatures below T_N. These are the same crystals described in previous work [9] and have dimensions $2\times3\times17\,mm^3$ and $2\times3\times25\,mm^3$. We looked for remnants of the S–P energy gap as well as evidence of excitations around the magnetic wave vector $Q=(0,1,\frac{1}{2})$. In both cases we were successful.

Our inelastic neutron experiments were performed at the IN12 triple-axis spectrometer at the ILL in Grenoble with an incident energy of 4.95 meV (vanadium width of 0.04 meV) and reactor to detector in-plane collimation of 33′-43′-43′-60′ with a Be filter placed in front of the sample. An orange cryostat was used over the range from 1.5 K to well above the spin–Peierls transition temperatures. We took measurements in the $(0,k,l)$ plane, mainly around the magnetic Bragg position at $Q=(0,1,\frac{1}{2})$.

Some elastic neutron data included here was taken at the DR3 reactor cold source at Risø National Laboratory on the TAS VI triple-axis spectrometer with an incident energy of 14.56 meV. Measurement was in the (h,k,h) direction in order to allow access to the structural superlattice peak at $Q=(\frac{1}{2},3,\frac{1}{2})$.

3. Results and discussion

To characterise the samples, sections of the crystals were used for magnetic susceptibility measurements with a SQUID magnetometer from 2 to 30 K in an applied field of 0.01 T with the c-axis of the crystal parallel to the field. The results are shown in Fig. 1 together with data from a pure sample of $CuGeO_3$ for comparison. The suppression of the spin–Peierls transition is apparent from the temperature dependence of the exponential decrease below T_{sp}. However, the transition to the 3D antiferromagnetic state cannot be seen in this orientation.

Further characterisation came from elastic neutron scattering measurements of the magnetic Bragg peak at $Q=(0,1,\frac{1}{2})$ and the superlattice peak at $(\frac{1}{2},3,\frac{1}{2})$.

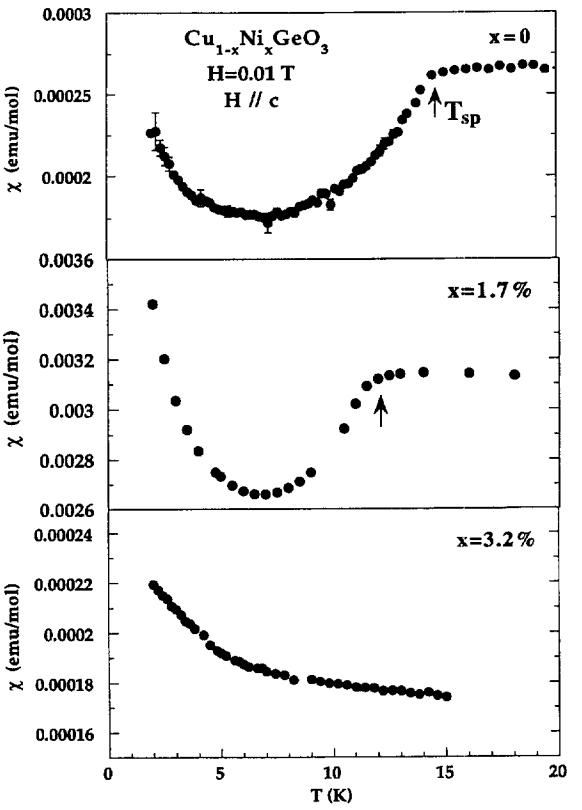

Fig. 1. Low-temperature DC susceptibility for $CuGeO_3$, $Cu_{0.983}Ni_{0.017}GeO_3$ and $Cu_{0.967}Ni_{0.032}GeO_3$ in a field of 0.01 T directed along the c-axis. The arrows indicate T_{sp} for the pure and 1.7% doped crystals.

Fig. 2(a) shows the temperature dependence of the integrated intensity of the magnetic peak for both doped crystals. Fitting with straight lines gives the transition temperatures T_N which are 2.0 and 4.2 K for the 1.7% and 3.2% Ni-doped crystals, respectively. Comparison of the relative intensities of the magnetic peak at $(0, 1, \frac{1}{2})$ for both crystals in Fig. 2(a), when normalised to monitor and volume, show that the more highly doped crystal has a more intense magnetic peak and has a higher Néel temperature. Both crystals exhibit a sharp increase in intensity below T_N and the magnetic moment is not saturated within the temperature range over which measurements were made. Comparing the integrated intensity of the magnetic reflection at $(0, 1, \frac{1}{2})$ and 1.5 K to the nuclear peak at $(0, 2, 0)$ and using the fact that the moment direction for Ni-doped crystals is along the $a*$-axis, a rough estimate of the magnetic moments, extrapolated to $Q = 0$ with the form factor curve for the Cu^{2+} free ion can be obtained. For the 3.2% Ni-doped crystal the effective moment $\mu_{eff} = g\mu_B S$ is calculated to be $0.16 \pm 0.03\mu_B$ while this decreases to $0.06 \pm 0.03\mu_B$ for the 1.7% Ni-doped sample. These values are slightly smaller than the calculated moments for Zn-doped crystals (3.2% Zn ($0.2\mu_B$) [12] and 3.4% Zn ($0.21\mu_B$) [11]).

Fig. 2(b) depicts the coexistence of the AF and dimerised phases in the 1.7% Ni-doped crystal. This can be seen from the strong remnant intensity of the superlattice reflection at temperatures where the magnetic peak becomes influential. Fitting with a power-law curve to the 1.7% Ni-doped data gave $T_{sp} = 11.5$ K while an absence of intensity at $(\frac{1}{2}, 3, \frac{1}{2})$ in the 3.2% Ni-doped crystal means there is no discernable transition to the S–P state.

In Fig. 2(c) the $(\frac{1}{2}, 3, \frac{1}{2})$ reflection for the 1.7% Ni-doped crystal is also compared with previous data on a pure $CuGeO_3$ crystal taken with an incident energy of 4.95 meV at Risø. The superlattice reflection in the doped compound clearly flattens out below 6 K, heralding the onset of detectable long-range antiferromagnetism at $T_N = 2.0$ K.

In an earlier experiment on a 2.9% Ni-doped crystal (with $T_{sp} = 9.2$ K) we used X-rays to measure the temperature dependence of the Bragg peak at the position (3.5, 1, 2.5) [13]. At the lowest achievable temperature, 3 K, the intensity of the (3.5, 1, 2.5) peak had diminished by 25%, not by 100% as might be expected for a complete phase transition. A simple coexistence model pictures the doped crystal as many regions of finite S–P chains, separated by Ni^{2+} ions with unpaired spins. These chain ends can act independently of the rest of the system; in particular, they can interact antiferromagnetically, producing long-range order over the entire crystal.

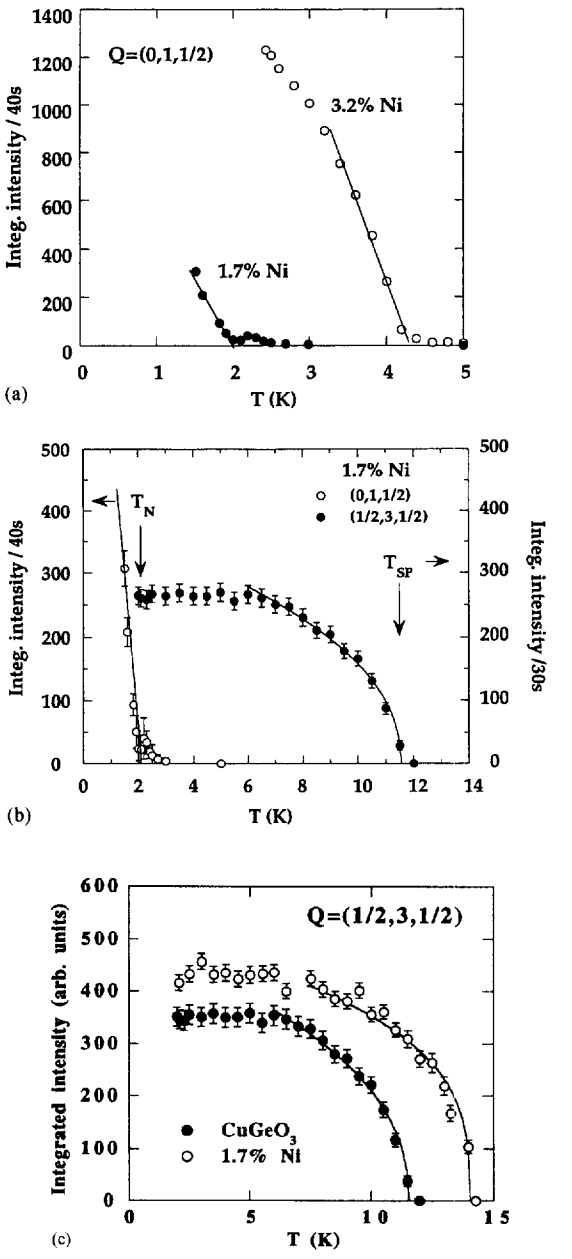

We used inelastic neutron scattering on the 1.7% Ni-doped crystal to investigate the existence of the S–P energy gap at the antiferromagnetic zone centre, $Q=(0,1,\frac{1}{2})$. A series of scans traced out the temperature dependence of this characteristic peak and are shown in Fig. 3 where they are fitted with Gaussian curves. We are confident that the position of the energy gap has been measured accurately because for each scan the quasi-elastic peak was symmetric and centred at $\Delta E=0$. From Fig. 3 it can be seen that the inelastic peaks are not resolution limited at these small energy transfer values. The most intense excitation at 1.5 K can be fitted well with a Gaussian at the position $\Delta E=1.7$ meV. The intensity of the S–P energy gap peak in the 1.7% Ni-doped crystal is much smaller than the corresponding intensity from our previous measurements on pure $CuGeO_3$ [14]. The ratio of the intensity of the energy gap peak to the peak at $\Delta E=0$ is 25% in the pure crystal, but only 0.1% in the doped crystal, which is probably why it has not been widely observed before.

Another significant point is that the S–P energy gap is clearly present at 1.5 K, a temperature below $T_N=2.1$ K. Therefore there is coexistence of the spin–Peierls phase with long-range antiferromagnetic order.

Fig. 4 shows the temperature dependence of the value of the energy gap for the pure and 1.7% Ni-doped crystals. They are fitted with a power-law relation for temperatures between 4 and 15 K:

$$\Delta E(T)=\Delta E(0)\left(1-\frac{T_{sp}}{T}\right)^{\beta} \quad (1)$$

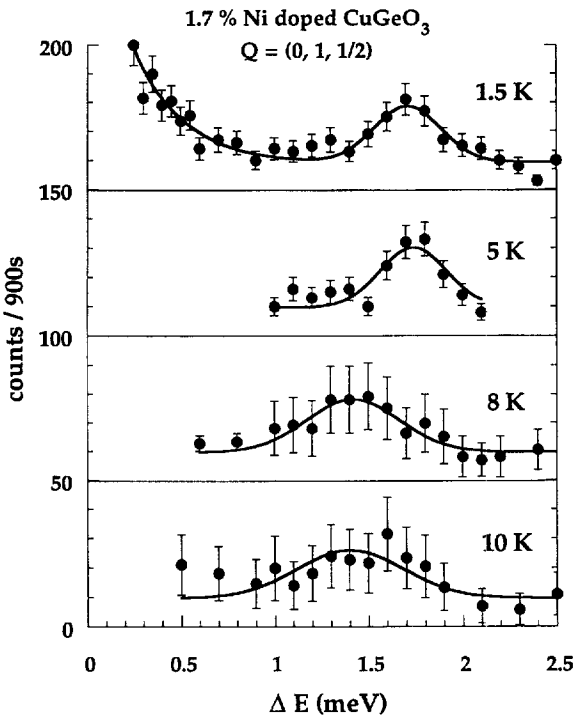

Fig. 3. Inelastic scans at $Q=(0,1,\frac{1}{2})$ for the 1.7% Ni-doped crystal at four different temperatures, showing how the spin–Peierls energy gap at 1.7 meV diminishes and moves closer to the elastic peak at $\Delta E=0$ as the temperature approaches $T_{sp}=11.5$ K. The data points have been fitted using a Gaussian with the background held constant.

Fig. 2. (a) Comparison of the 1.7% and 3.2% Ni order parameters at $Q=(0,1,\frac{1}{2})$, obtained by neutron diffraction. The straight-line fits were used to obtain T_N. (b) Temperature dependence of the peak intensities at the magnetic position $Q=(0,1,\frac{1}{2})$ and at the dimerisation wave vector $Q=(\frac{1}{2},3,\frac{1}{2})$ for the 1.7% Ni-doped crystal of $CuGeO_3$. The $(\frac{1}{2},3,\frac{1}{2})$ data points have been fitted with a power-law curve that shows T_{sp}. (c) Comparison of the $(\frac{1}{2},3,\frac{1}{2})$ superlattice reflection for pure $CuGeO_3$ with the 1.7% Ni-doped crystal. The drop in intensity below 6 K for the doped compound is a precursor to the antiferromagnetic order that appears below 2 K. Data at the $(0,1,\frac{1}{2})$ position for the 1.7% Ni-doped crystal was measured at IN12; all other data was taken at TAS VI at Risø. Intensities have been adjusted for sample volumes but no correction has been made for differences in flux at the different instruments.

with $\beta=0.11\pm0.05$ for both pure and doped compounds. This evidence that the energy gap in the doped crystal has the same evolution with temperature as pure $CuGeO_3$ can be seen more clearly in the inset of Fig. 4 in which $\Delta E/T_{sp}$ is plotted against the reduced temperature. While the temperature dependence of the order parameter for the 1.7% Ni-doped crystal is very similar to $CuGeO_3$, the transition temperature is lower and the limiting value $\Delta E\rightarrow 1.7$ meV as $T\rightarrow 0$. These factors suggest that the system consists of a modified S–P phase, that is that the magnetic ions do affect the spin–Peierls gap, rather than merely subdividing the crystal into S–P regions which act independently. If there were no finite size effects, the position of the gap would be unchanged at $\Delta E=1.95$ meV and solely the intensity of this inelastic peak would diminish with doping.

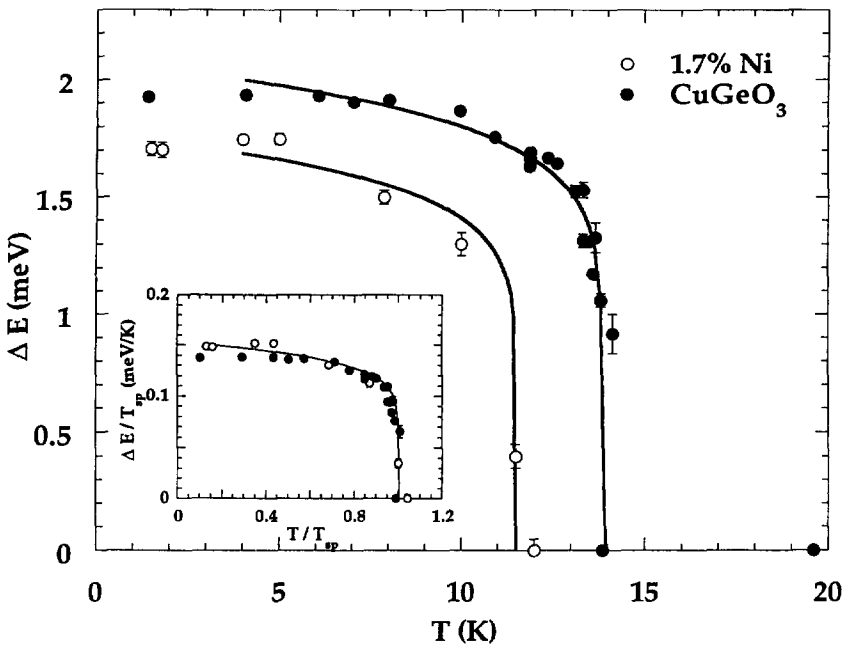

Fig. 4. Comparison of the temperature dependence of the S–P energy gap for pure $CuGeO_3$ and 1.7% Ni-doped $CuGeO_3$. The data points are fitted with a power-law curve described in the text.

Inelastic measurements on a crystal with nearly twice the dopant concentration, 3.2% Ni, found the S–P gap had collapsed almost completely. At this concentration, if the position and intensity of the energy gap diminishes in a linear manner with x (like T_{sp} for $x \leqslant 5\%$ [9]), then it would be very faint and situated at approximately $\Delta E = 1.3$ meV. Fig. 5 shows increased background for the energy transfer range above the magnetic excitation at 0.4 meV, but unfortunately our statistics are not good enough to resolve any excitation at this $(Q, \Delta E)$ position.

In line with the transition to the Néel state in the 1.7% Ni-doped crystal, we expected that additional low-lying magnetic excitations would be observable by inelastic neutron scattering. Regnault et al. [15] had measured a weak magnon signature at low energies in a 0.7% Si-doped crystal. Extra inelastic peaks have also been observed in two Zn-doped crystals [12]; and ESR measurements found antiferromagnetic resonances below T_N in Zn-doped crystals of $CuGeO_3$ [16, 17]. However, no excitation below $\Delta E = 0.5$ meV could be resolved from our neutron scattering measurements on the 1.7% Ni-doped

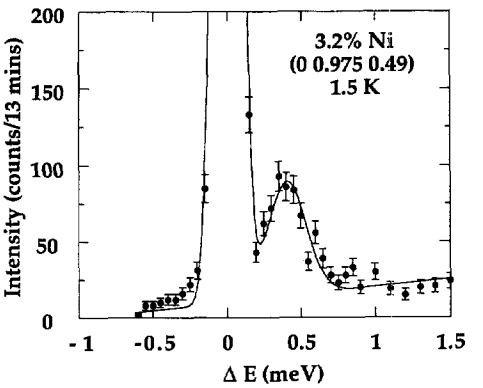

Fig. 5. 3.2% Ni-doped crystal – an inelastic scan at $(0, 0.975, 0.49)$ showing the magnetic excitation at $\Delta E = 0.4$ meV.

crystal. The strong Bragg peak at $Q = (0, 1, \frac{1}{2})$ has a width in ΔE, due to the tail of the resolution ellipse passing through the Bragg peak, that masks any inelastic excitations close to this position. Even at high temperatures there is a contribution.

The next set of measurements used a 3.2% Ni-doped crystal which has a higher T_N (4.2 K) than the

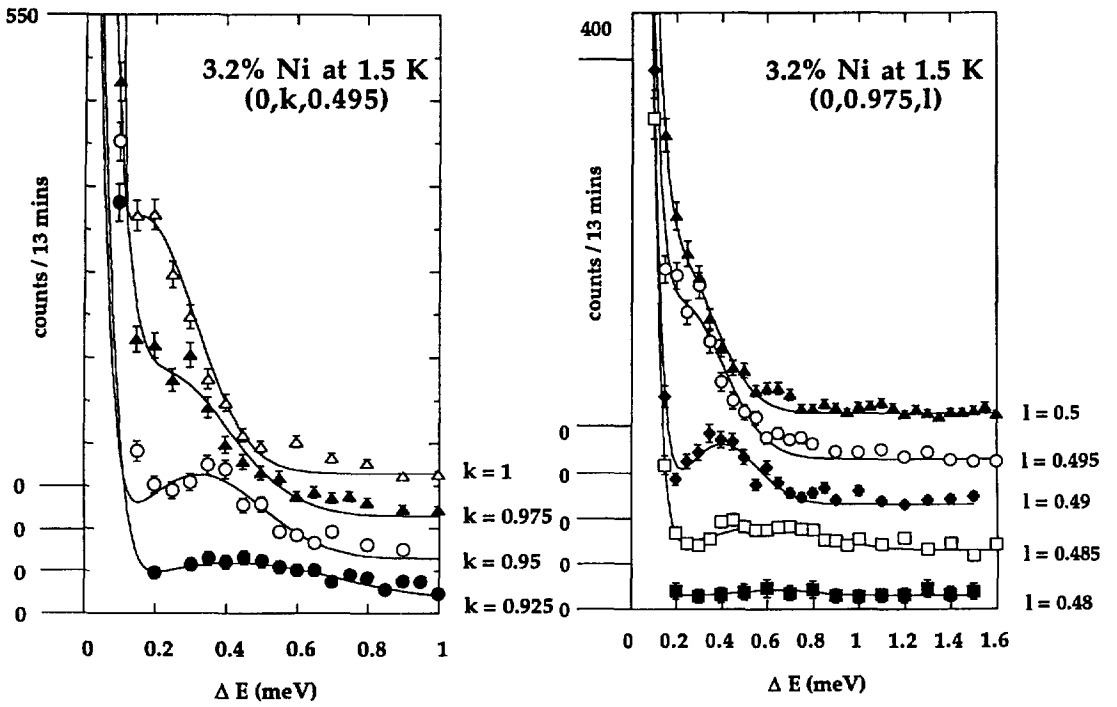

Fig. 6. Plots of constant Q scans along (a) the b-axis and (b) the c-axis for the 3.2% Ni-doped crystal of $CuGeO_3$ at 1.5 K. Each set of points has been fitted with two Gaussians, one centred at $\Delta E = 0$ and a second one for the magnetic excitation at larger energy transfer. The scans are superimposed with each spectrum shifted vertically by 50 counts.

1.7% Ni-doped sample. Therefore, measurements at 1.5 K should be low enough in temperature so that the order parameter is fully saturated. The postulated magnetic excitation would then be intense and distinctly separate from the $\Delta E = 0$ position.

However, this excitation could not be resolved at the wave vector $(0, 1, \frac{1}{2})$ as it was still masked by the magnetic/quasi-elastic contribution. Therefore, $Q = (0, 0.975, 0.49)$ was chosen as a position which is so close to the $(0, 1, \frac{1}{2})$ wave vector that magnetic excitations along k and l will not have dispersed significantly.

At $Q = (0, 0.975, 0.49)$ we observed a peak centred at $\Delta E = 0.4$ meV at 1.5 K (Fig. 5). A series of inelastic scans were taken at various wave vectors, all at 1.5 K, in order to map out the dispersion curves along the $(0, k, 0.49)$ and $(0, 0.975, l)$ directions. The scans are depicted in Figs. 6(a) and (b) with Gaussians fitted both to the Bragg peak at $\Delta E = 0$ and to the magnetic excitation.

Note how the excitation moves to higher energies and also how the intensity decreases rapidly with only a very small increment in q_k or q_l. The FWHM of the excitation remained constant at ≈ 0.25 meV in both k and l directions until $k = 0.925$ and $l = 0.485$. At these values it broadened, becoming indistinct. At higher Δq values the excitation could not be distinguished from the background.

The dispersion of the magnetic excitation in the k and l directions for the 3.2% Ni-doped crystal are shown in Figs. 7(a) and (b), with points taken from fits to the plots in Fig. 6. Data taken by Nishi [3] on a pure crystal of $CuGeO_3$ are also included for comparison. Peak intensities in the doped crystal diminish very rapidly with distance from the zone centre, therefore we have only a cluster of points with low momentum transfer and further experiments will extend these dispersion curves. Nevertheless, a clear difference between the k and l directions can be seen from Fig. 8 where the points are fitted with dispersion relations

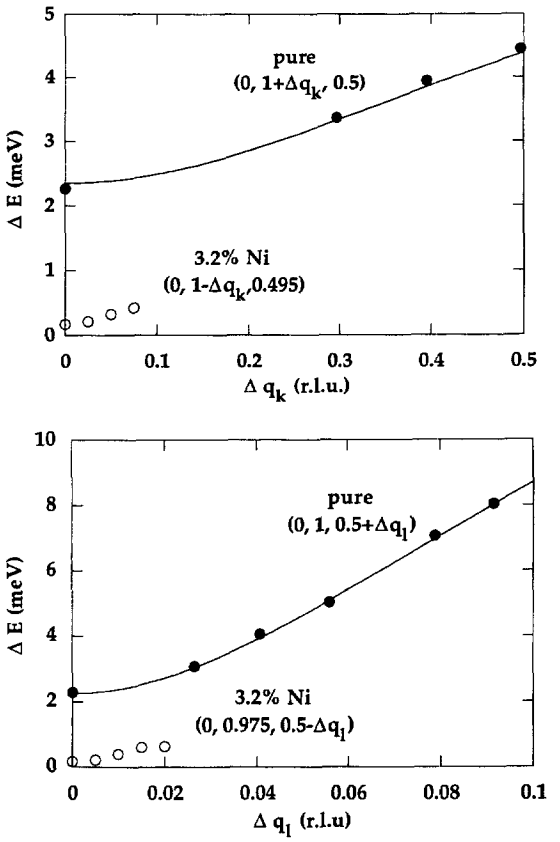

Fig. 7. Dispersion relation of magnetic excitations along (a) $(0, 1-\Delta q_k, 0.495)$ and (b) $(0, 0.975, 0.5-\Delta q_l)$ for the 3.2% Ni-doped crystal. Data points taken by Nishi et al. [3] for a pure crystal of $CuGeO_3$ have been included for comparison and fitted with equations (see text) for a 3D antiferromagnet with an anisotropy gap.

arising from the Heisenberg spin wave theory for an antiferromagnetic system with an anisotropy gap,

$$\omega(q_b) = \sqrt{\Delta^2 + (\gamma_b)^2 \sin^2\left(\frac{\pi}{2} \cdot q_b\right)}, \tag{2}$$

$$\omega(q_c) = \sqrt{\Delta^2 + (\gamma_c)^2 \sin^2(2\pi \cdot q_c)}. \tag{3}$$

Here Δ is the anisotropy gap for a magnetic system which can be compared with the spin–Peierls energy gap of 1.95 meV in $CuGeO_3$. γ_b and γ_c are variables that depend on the exchange parameters J_b and J_c along the b- and c-axis, respectively. These are the

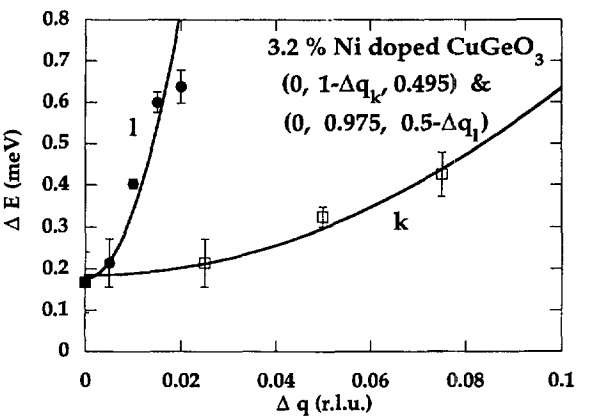

Fig. 8. Dispersion curves along the k and l directions for the 3.2% Ni-doped crystal presented with the same x-axis (Δq) where the shift in q is from the position $Q = (0, 0.975, 0.495)$. The curves are fitted with equations for a 3D antiferromagnet with an anisotropy gap.

same type of equations that were used to fit dispersion of the spin–Peierls energy gap along the b-axis in pure $CuGeO_3$ by Nishi et al. [3] and Regnault et al. [18]. In other words a 1D antiferromagnet with alternation in the intrachain exchange coefficients can be modelled equally well by simple AF ordering with anisotropy along one axis [19].

Fitting to the pure $CuGeO_3$ data in Figs. 7(a) and (b) gives $J_c = 5.04 \pm 0.06$ meV and $\alpha = 0.93 \pm 0.02$, where $\alpha = J'/J$ is the alternation parameter which is 1 for a uniform system and 0 for a state of complete dimerisation. These values are reasonably close to results published by Nishi et al. ($2J_c = 10.4$ meV and $\alpha = 0.78$) [3, 20].

Unfortunately, there are too few points on the dispersion curves for the magnetic excitation in the 3.2% Ni-doped crystal to be able to extract exchange parameters from the fitted curves with any real degree of certainty. The only conclusions available from these preliminary results are (i) the exchange coefficients $J_b* = 0.7 \pm 0.1$ meV and $J_c* = 1.8 \pm 0.3$ meV in the doped crystal are much smaller than J_b and J_c in the pure crystal; (ii) the value of $\alpha = 0.98 \pm 0.08$ is higher, therefore dimerisation has decreased; and (iii) there is still considerable anisotropy along the b and c directions in the 3D antiferromagnetic low-temperature phase of Ni-doped $CuGeO_3$, although the effect is smaller than

in the quasi-1D spin–Peierls phase. Other quasi-1D antiferromagnets containing Cu^{2+} such as Li_2CuO_2 [21] and $MgCu_2O_3$ [22] which undergo transitions to 3D antiferromagnetic order at 9 K and 95 K respectively, exhibit much greater anisotropy between hard and easy axes in the long-range ordered phase.

Cowley et al. [19] describe a situation where the ground state is neither completely a spin–Peierls or an ordered antiferromagnetic state but a combination of them both. In this case there is a weak antiferromagnetic moment that transforms the degenerate triplet excited states of the spin–Peierls phase into two transverse spin waves and a longitudinal mode. Given that we know the S–P phase is still partially active (from the remnant intensity of the superlattice peak at $(\frac{1}{2}, 3, \frac{1}{2})$ and that the moment ($0.24\mu_B$ in a 2.4% Zn doped crystal) [9] is less than expected for an antiferromagnet composed of Cu^{2+} spins; we feel this explanation is the most plausible. We await future experimental and theoretical results for further explanation of this scenario.

In conclusion, we have examined two different crystals of $CuGeO_3$ doped with 1.7% and 3.2% Ni, and utilised high-resolution inelastic neutron scattering to observe a remnant spin–Peierls energy gap and also a low-lying magnetic excitation, confirming the coexistence of the antiferromagnetic and dimerised phases in doped $CuGeO_3$.

Acknowledgements

Many of the results presented here were measured at IN12 at the Institut Laue-Langevin. We would like to acknowledge the Chemistry Department at Risø for providing time on their mass spectrometer, while the Interdisciplinary Research Centre at Cambridge generously allowed us to use their SQUID. Work at Warwick was funded by the EPSRC.

References

[1] M. Hase, I. Terasaki, K. Uchinokura, Phys. Rev. Lett. 70 (1993) 3651.
[2] K. Hirota, D. Cox, J. Lorenzo, G. Shirane, J. Tranquada, M. Hase, K. Uchinokura, H. Kojima, Y. Shibuya, I. Tanaka, Phys. Rev. Lett. 73 (1994) 786.
[3] M. Nishi, O. Fujita, K. Akimitsu, Phys. Rev. B 50 (1994) 6508.
[4] O. Fujita, T. Akimitsu, M. Nishi, K. Kakurai, Phys. Rev. Lett. 74 (1995) 1677.
[5] J.-P. Renard, K. Le Dang, P. Veillet, G. Dhalenne, A. Revcolevschi, L.-P. Regnault, Europhys. Lett. 30 (1995) 475.
[6] L.P. Regnault, M. Ain, B. Hennion, G. Dhalenne, A. Revcolevschi, Physica B 213&214 (1995) 278.
[7] M. Weiden, W. Richter, C. Geibel, F. Steglich, P. Lemmens, B. Eisener, M. Brinkmann, G. Guntherodt, Physica B 225 (1996) 177.
[8] J.-G. Lussier, S. Coad, D. McMorrow, D. Paul, J. Phys. Condens. Matter 7 (1995) L325.
[9] S. Coad, J.-G. Lussier, D. McMorrow, D. Paul, J. Phys. Condens. Matter 8 (1996) 6251.
[10] N. Koide, Y. Sasago, T. Masuda, K. Uchinokura, Czech J. Phys. 46 S4 (1996) 1981.
[11] M. Hase, K. Uchinokura, R. Birgeneau, K. Hirota, G. Shirane, J. Phys. Soc. Japan 65 (1996) 1392.
[12] Y. Sasago, N. Koide, K. Uchinokura, M. Martin, M. Hase, K. Hirota, G. Shirane, Phys. Rev. B 54 (1996) R6835.
[13] V. Kiryukhin, B. Keimer, J. Hill, S. Coad, D. McK. Paul, Phys. Rev. B 54 (1996) 7269.
[14] J.-G. Lussier, S. Coad, D. McMorrow, D. Paul, J. Phys. Condens. Matter 8 (1996) L59.
[15] L. Regnault, J. Renard, G. Dhalenne, A. Revcolevschi, Europhys. Lett. 32 (1995) 579.
[16] A. Smirnov, V. Glazkov, A. Vasilev, L. Leonyuk, S. Coad, D. Paul, JETP Lett. 64 (1996) 305.
[17] M. Hase, M. Hagiwara, K. Katsumata, Phys. Rev. B 54 (1996) R3722.
[18] L.P. Regnault, M. Ain, B. Hennion, G. Dhalenne, B. Revcolevschi, Phys. Rev. B 53 (1996) 5579.
[19] R.A. Cowley, B. Lake, D.A. Tennant, J. Phys. Condens. Matter 8 (1996) L179.
[20] M. Nishi, O. Fujita, J. Akimitsu, K. Kakurai, Y. Fujii, Physica B 213 & 214 (1995) 275.
[21] H. Ohta, N. Yamauchi, T. Nanba, M. Motokawa, S. Kawamata, K. Okuda, J. Phys. Soc. Japan 62 (1993) 785.
[22] M. Winkelmann, H.A. Graf, N.H. Andersen, Phys. Rev. B 49 (1994) 310.